Least squares spectral resolution of liquid chromatography–mass spectrometry data of glycerophospholipids

ARTICLE *in* JOURNAL OF CHROMATOGRAPHY A · JANUARY 2013

Impact Factor: 4.17 · DOI: 10.1016/j.chroma.2012.12.070 · Source: PubMed

5 AUTHORS, INCLUDING:

Ying-Xu Zeng

University of Bergen

14 PUBLICATIONS **136** CITATIONS

SEE PROFILE

Sonnich Meier

Institute of Marine Research in Norway

49 PUBLICATIONS **937** CITATIONS

SEE PROFILE

Journal of Chromatography A, 1280 (2013) 23–34

Contents lists available at SciVerse ScienceDirect

Journal of Chromatography A

journal homepage: www.elsevier.com/locate/chroma

Least squares spectral resolution of liquid chromatography–mass spectrometry data of glycerophospholipids

Ying-Xu Zeng[a], Svein A. Mjøs[a,*], Sonnich Meier[b], Chen-Chen Lin[a], Reidun Vadla[a,b]

[a] Department of Chemistry, University of Bergen, P.O. Box 7803, N-5020 Bergen, Norway
[b] Institute of Marine Research, P.O. Box 1870 Nordnes, NO-5817 Bergen, Norway

ARTICLE INFO

Article history:
Received 4 July 2012
Received in revised form
20 December 2012
Accepted 26 December 2012
Available online 9 January 2013

Keywords:
Glycerophospholipids
Phosphatidylcholine
Phosphatidylethanolamine
Sphingomyelins
LC–MS
Least squares spectral resolution

ABSTRACT

Liquid chromatography–mass spectrometry represents a powerful tool for the analysis of intact glycerophospholipids (GPLs), but manual data interpretation may be a bottleneck in these analyses. The present paper proposes a least square regression approach for the automated characterization and deconvolution of the main GPLs species, *i.e.*, phosphatidylcholine and phosphatidylethanolamine analyzed by class-specific scanning methods such as precursor ion scanning and neutral loss scanning, respectively. The algorithm is based on least squares resolution of spectra and chromatograms from theoretically calculated mass spectra, and eliminates the need for isotope correction. Results from the application of the methodology on reference compounds and extracts of cod brain and mouse brain are presented.

1. Introduction

Glycerophospholipids (GPLs) are the building blocks of cell membranes that are present in all organisms. They are dynamically involved in many important biological functions and processes such as membrane trafficking, cellular signaling and metabolic regulation [1]. An increasing body of evidence suggests that the chemical diversity and composition of GPLs are correlated to certain diseases, such as Alzheimer's disease [2] and other neural disorders [3], cardiovascular disease, and immunological abnormalities [4].

GPLs can be classified into several classes according to the polar head group linked to the phosphate group at the *sn*-3 position of the glycerol backbone. Among these classes phosphatidylcholine (PC) and phosphatidylethanolamine (PE) are the dominant species in most eukaryotic membranes, present in about 3:2 molar ratio and constitute around 75 mol% of total GPLs [5]. They can be further defined by different combinations of fatty acids with various carbon numbers and double bounds, esterified at the *sn*-1 and *sn*-2 positions of the backbone, thus resulting in a large number of PC and PE molecular species. Since the roles of GPLs in cellular biochemistry are still only partly understood, great efforts have been initiated with focus on the systematic analyses of GPLs and with emphasis on the major PC and PE species in order to provide insights into the biological and physiological functions of the GPLs in biological systems.

Many indirect and direct approaches have been used for the analysis of PC and PE molecular species. The former normally consist of separation of PC and PE by thin layer chromatography (TLC), liquid chromatography (LC) or solid phase extraction (SPE), followed by derivatization of individual fatty acids in the different lipid classes and quantification by gas chromatography (GC). The main disadvantages of these indirect approaches not only lie in multiple laborious steps involved, poor resolution and reproducibility along with possible oxidation of the fatty acids, but also in the inability of providing structural information of intact PC and PE species [6]. On the other hand, direct approaches utilizing high performance liquid chromatography (HPLC) coupled to various detectors such as ultraviolet (UV), evaporative light-scattering detectors (ELSD) and mass spectrometry (MS), are today widely employed due to their capability of analyzing the intact PC and PE species [7–9]. Advances in soft ionization techniques such as electrospray ionization (ESI) have led to rapid progress in MS-based approaches including the direct infusion technique (shotgun lipidomics) and liquid chromatography coupled to MS (LC–MS), making them popular lipidomic platforms [10]. In particular, the GPLs class-specific MS profiling method is advantageous because it allows the specific detection of various GPLs classes based on their fragmentation mechanisms with high selectivity and

* Corresponding author. Tel.: +47 5558 3553; fax: +47 5558 9490.
E-mail address: svein.mjos@kj.uib.no (S.A. Mjøs).

0021-9673/$ – see front matter © 2013 Elsevier B.V. All rights reserved.
http://dx.doi.org/10.1016/j.chroma.2012.12.070

sensitivity. For example, by using precursor ion scanning (PIS) of m/z 184 with positive ionization on a triple quadrupole instrument, all the PC species can be detected since the phosphocholine head group is normally lost as a charged fragment, while by using neutral loss scanning (NLS) of m/z 141 with positive ionization, all the PE species can be monitored since the phosphoethanolamine head group is lost as a neutral fragment [1,11–13].

As these MS-based approaches become increasingly favored, data interpretation is becoming a bottleneck of lipidomic studies due to the huge amounts of data produced and the inherent complexity of biological samples, which requires extensive manual work. There are only a few computational tools available to assist the rapid and automated lipidomic data analysis process. Current computational tools can be generally classified into two groups according to the lipidomic platforms used, *i.e.*, MS profiling group and LC–MS group. The former is based on shotgun approach only, where different algorithms are specifically designed for different types of datasets acquired by various MS instruments [14–18]. Compared to the MS profiling group, few algorithms are available for LC–MS data even though the LC–MS approach has some substantial advantages over shotgun MS concerning accurate identification, quantitation, reduced ion suppression and assignment of acyl chains [19]. The available LC–MS based algorithms have various functions directing at different types of molecules, but few take full advantage of the chromatographic separation since they are either based on extracting the mass spectra as input or on extracting chromatograms for identification and quantification [20–23]. In general, the available algorithms do not provide an efficient solution for fully utilizing the useful chromatographic and mass spectral information derived from the LC–MS based data.

In the present study, a novel approach is proposed for spectral deconvolution, identification and quantification of the molecular PC and PE species in LC–MS data acquired by PIS and NLS modes. The approach is based on calculation of theoretical mass spectra of possible PC and PE compounds from a list of fatty acids followed by resolution of the sum spectrum and the full chromatographic profile by least squares regression. Since the theoretical spectra contain the isotope pattern of the individual compounds, there is no need for additional isotope correction. The principle and the algorithm are described in the theory section below. The performance of the developed algorithm was tested by using both standard mixtures and extracts of brain lipids and the results demonstrate that it is an efficient tool in lipidomic data analysis.

2. Theory

2.1. Nomenclature

In the following theory section and elsewhere in the manuscript, standard matrix notation is applied, where scalar values are denoted by lower case letters in italics, vectors are denoted by bold lower case letters and matrices are denoted by bold uppercase letters. Superscript 'T' on a matrix indicates that it is transposed, while superscript 'T' on a vector denotes that it is treated as a row vector. Scalars are denoted by lower case letters in italics.

Phospholipids are referred to by the lipid class (PE or PC) followed by total number of carbon atoms and total number of double bonds in the two fatty acids in the molecule. The two hydroxy groups in the phospholipid molecules that are linked to fatty acids are denoted by the stereospecific numbering, *sn*-1 and *sn*-2 [24]. Fatty acids are referred to by total number of carbon atoms followed by the total number of double bonds, and optionally the position of the double bond counted from the methyl end of the molecule [24]. Plasmalogens are similar in structure to ordinary PC and PE, but with a vinyl-ether linked hydrocarbon chain in the *sn*-1 position. Plasmalogens are denoted by the total number of carbon atoms followed by total number of double bonds in the fatty acid and hydrocarbon chain, excluding the double bond in the vinyl-ether group. Sphingomyelins (SM) are molecules based on a sphingoid base where a fatty acid is bound to the amino-group in the 2-position via an amide bond, and phosphocholine is linked to the hydroxy-group in the 1-position. SM are denoted by the total number of carbon atoms followed by total number of double bonds in the fatty acid and the sphingoid base.

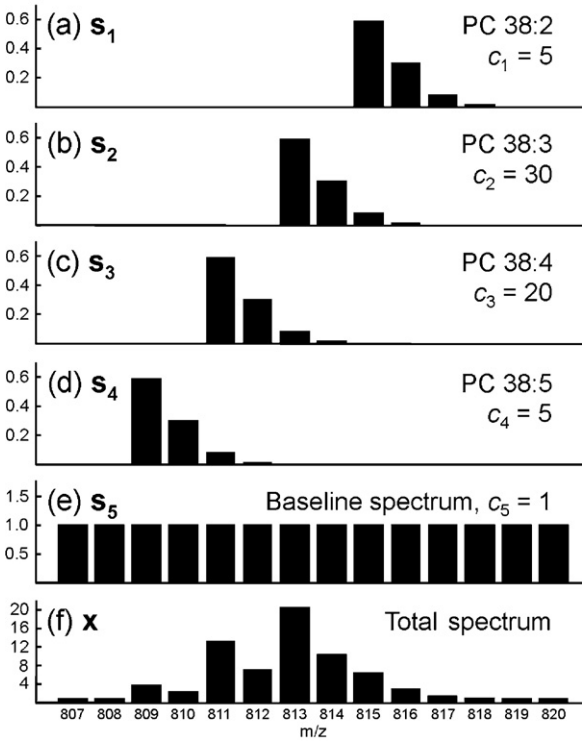

Fig. 1. Simulated unit-resolution PIS mass spectra (a) PC 38:2, (b) PC 38:3, (c) PC 38:4, (d) PC 38:5, (e) baseline spectrum and (f) total spectrum generated from (a)–(e). See Section 2.1 for lipid nomenclature.

2.2. Principle

Fig. 1a–d shows simulated unit-resolution PIS mass spectra of PC species with 38 carbon atoms and 2–5 double bonds in the fatty acid chains. The lightest ions in each spectrum, corresponding to the nominal mass of $[MH]^+$, constitute approximately 59% of the signal, while the masses of $[MH+1]^+$, $[MH+2]^+$, $[MH+3]^+$ and $[MH+4]^+$ account for approximately 30%, 8.6%, 1.7% and 0.2%, respectively. These ratios will vary slightly with molecular composition. Fatty acids typically have from 12 to 24 carbon atoms and the resulting PC molecules will therefore have from 24 to 48 carbon atoms. $[MH]^+$ will account for 69% and 53% of the signal in PC 24:0 and 48:0, respectively.

It can be seen from the figure that there is overlap between the isotope patterns of the different PC species. The $[MH]^+$ signal will be influenced by $[MH+2]^+$ from a compound with one more double bond, and the $[MH+2]^+$ signal will be influenced by the $[MH]^+$ signal from a compound with one less double bond. $[MH+3]^+$ and $[MH+4]^+$ also interfere with other signals, but these are of less importance. Different isotope correction strategies have been proposed to correct for the overlap of isotope patterns [16,20,23].

In addition to the contribution from the different molecular species, a mass spectrum may also have a baseline resulting from noise contributions, especially if it is averaged from a large number

of scans. This is illustrated in Fig. 1e, where the baseline is equal on all masses.

When a total mass spectrum, $\mathbf{x}^T$, has contributions from several compounds, the signal is a result of the concentration of the individual compounds, c, multiplied with the corresponding normalized mass spectra, $\mathbf{s}^T$, as shown in Eq. (1).

$$\mathbf{x}^T = \mathbf{s}_1^T \cdot c_1 + \mathbf{s}_2^T \cdot c_2 + \cdots + \mathbf{s}_n^T \cdot c_n \quad (1)$$

The concentrations, c, will be 'pseudo concentrations', since different compounds will have different response factors and effects such as ion suppression may lead to synergistic interactions between the different compounds. For the sake of simplicity, c is referred to as concentration, with reference to the measured signal. The hypothetical spectrum $\mathbf{x}^T$ generated from the individual spectra and concentrations varying from 5 to 30, and with a baseline level of 1, is shown in Fig. 1f.

If the relative distributions of the masses in the spectra are known, it is possible to find the concentrations of the individual compounds, c, from the total spectrum, $\mathbf{x}^T$, by least squares regression according to Eq. (2).

$$\mathbf{c} = \mathbf{x}^T\mathbf{S}(\mathbf{S}^T\mathbf{S})^{-1} \quad (2)$$

where $\mathbf{S}^T$ is an $m \times n$ matrix holding the m individual spectra of n ions, and $\mathbf{c}$ will be a vector of the m concentrations. As long as the individual spectra in $\mathbf{S}^T$ are normalized to sum = 1 (L1-normalization), the regression coefficients in $\mathbf{c}$ will be a direct estimate of the total signal from the corresponding compounds. When the baseline spectrum is described by a vector of ones, the regression coefficient for the baseline will be a direct estimate of the average baseline level of each individual ion.

In a case where all spectra in $\mathbf{S}^T$ are unique and none of the spectra can be explained by linear combination of other spectra in $\mathbf{S}^T$, Eq. (2) will give a unique solution from $\mathbf{x}^T$ and $\mathbf{S}^T$ if there is no noise in the system. These criteria are fulfilled for PIS and NLS spectra of PC and PE as long as the fatty acids are even-numbered and there are less than 14 double bonds in the two fatty acid chains. Docosahexaenoic acid (22:6 n-3), which is the most unsaturated common fatty acid, has six double bonds, so the maximum total number of double bonds from common fatty acids in PC and PE molecules will be 12. However, if fatty acids with odd-numbered carbon chains are included there will be spectral similarities between compounds differing by one carbon and seven double bonds. Due to a different number of carbon atoms and hydrogen atoms, the spectra will not be identical, but the difference between them will be less than the noise that can be expected in any real system. In principle, the methodology described above is not limited to unit-resolution mass spectra, and a mass resolution of 0.1 Da or better would solve the problem.

2.3. Algorithm

A spectral resolution based on the principle described above will eliminate the need for isotope correction and baseline subtraction. Based on this principle the following algorithm for identification and quantification of PC and PE analyzed respectively by PIS and NLS was developed:

2.3.1. Calculation of sum spectrum $\boldsymbol{x}^T$

A sum spectrum, $\mathbf{x}^T$ is created from the entire raw data set or from a sub-section of an LC–MS chromatogram.

2.3.2. Calculation of possible compounds

From a list of common fatty acids molecular compositions of possible PC or PE species are calculated. In the same step, the equivalent carbon numbers (ECN) of the species are calculated. An option at this stage is to constrain the list of compounds to a certain range of ECN, which would be natural when $\mathbf{x}^T$ is from a sub-section of a chromatogram. At this stage it is also possible to add compounds in addition to the ordinary PC or PE species, such as other lipid classes or artifacts. The molecular composition of these lipids classes can be calculated from fatty acids, or molecules can be specified individually. In this work sphingomyelins was for instance added in one of the examples shown in the results section.

2.3.3. Generation of theoretical mass spectra, $\boldsymbol{S}^T$

From the molecular composition of step 2, the theoretical mass spectra resembling the isotope distributions are calculated and normalized to sum = 1. The spectra are calculated with a mass accuracy of four decimals and thereafter binned to a selected resolution (1 in this case). The spectra are stored in $\mathbf{S}^T$. Before the binning to unit resolution, it may be necessary to add a mass offset to the calculated spectra. With no offset, $[MH]^+$ of PC species with less than 28 carbon atoms and PE species with less than 31 carbon atoms will be rounded to even masses, while the other compounds will be rounded to odd masses. An offset of +0.1 Da for PC and +0.2 Da for PE will ensure that all compounds are rounded to odd masses, and an offset of −0.4 Da for PC and −0.3 Da for PE will ensure that all are rounded to even masses. Whether positive or negative offsets are used is irrelevant for the algorithm as long as the experimental data in $\mathbf{x}^T$ is treated in a similar way.

2.3.4. Deleting absent spectra from $\boldsymbol{S}^T$

Spectra in $\mathbf{S}^T$ where the most abundant ion ($[MH]^+$ in this case) is not present in $\mathbf{x}^T$ above a predefined threshold are regarded absent from the total spectrum. These are therefore deleted from $\mathbf{S}^T$.

2.3.5. Filter for spectral similarity

The remaining spectra in $\mathbf{S}^T$ are then checked for spectral similarity. As explained above, this filter is only necessary if fatty acids with odd number of carbon atoms are included in step 2. If the correlation coefficient between two spectra are above 0.9 and the two spectra stem from compounds with even and odd number of fatty acid carbon atoms, the spectrum from the compound with odd number of carbon atoms is deleted from $\mathbf{S}^T$. In this way, spectra that can only be explained by compounds having an odd number of carbon atoms are kept.

2.3.6. Addition of baseline

A baseline spectrum, which is a row vector of ones with the same number of columns as in $\mathbf{S}^T$ is added as the last row in $\mathbf{S}^T$. This step can be omitted if $\mathbf{x}^T$ is from baseline subtracted spectra or if the baseline for other reasons is insignificant.

2.3.7. Resolution

Prior to resolution, both $\mathbf{S}$ and $\mathbf{x}^T$ are constrained to contain only masses that are present in both. The concentrations of each of the compounds remaining in $\mathbf{S}^T$ are thereafter calculated by Eq. (2). When there is noise in $\mathbf{x}^T$, a large number of minor compounds may be found, and compounds may also have small negative values in $\mathbf{c}$. For the best results, it may therefore be necessary to do a recalculation after constraining $\mathbf{S}^T$ to compounds with concentrations above a certain level.

2.3.8. Validation

A validation spectrum $\mathbf{x}_{val}^T$ can be calculated from $\mathbf{S}^T$ and the calculated $\mathbf{c}$ according to Eq. (3).

$$\mathbf{x}_{val}^T = \mathbf{c} \times \mathbf{S}^T \quad (3)$$

$\mathbf{x}^T$ and $\mathbf{x}_{val}^T$ are thereafter compared. Any deviations between the two indicate that the resolution is inaccurate. Any ions that were above the threshold in step 4 and that are not among the ions in $\mathbf{S}^T$,

also indicate that there are compounds contributing to the original $\mathbf{x}^T$ that are not accounted for.

2.3.9. Chromatographic resolution

In cases where $\mathbf{x}^T$ stems from a chromatogram or from a section of a chromatogram, the results can also be validated by chromatographic resolution according to Eq. (4), which is the central equation in most multivariate techniques for chromatographic deconvolution based on spectral information [25].

$$\mathbf{C} = \mathbf{XS}(\mathbf{S}^T\mathbf{S})^{-1} \quad (4)$$

This equation is similar to Eq. (2), except that $\mathbf{X}$ is now a matrix of the two-dimensional raw data with number of rows corresponding to the number of scans (retention times) and number of columns corresponding to the number of ions in the mass spectra. $\mathbf{C}$ will then be a matrix holding the chromatographic profiles of each compound in $\mathbf{S}^T$ with number of rows corresponding to the number of scans and number of columns corresponding to the number of compounds. The resolved chromatographic profiles can be used to check that compounds with similar ECN values elute in the same regions (in reversed-phase LC).

Similar to the resolution by Eq. (2), a flat baseline spectrum can be added to $\mathbf{S}^T$ in Eq. (4). Any structure in the corresponding chromatographic profile indicates that there are peaks that are not accounted for. It can also be checked that the theoretical spectra, $\mathbf{S}^T$, and the resolved chromatograms, $\mathbf{C}$, explain the structure in $\mathbf{X}$ by calculating residuals according to Eq. (5).

$$\mathbf{R} = \mathbf{X} - \mathbf{CS}^T \quad (5)$$

Several fatty acid combinations may give PC and PE species with the same number of carbon atoms and double bonds, and the chromatograms in $\mathbf{C}$ may also be used to quantify these if there is sufficient chromatographic resolution.

3. Experimental

3.1. Standards and samples

PC and PE standards, including 1,2-didocosahexaenoyl-*sn*-glycero-3-phosphocholine (PC 22:6/22:6), 1-palmitoyl-2-docosahexaenoyl-*sn*-glycero-3-phosphocholine (PC 16:0/22:6), 1-palmitoyl-2-arachidonoyl-*sn*-glycero-3-phosphocholine (PC 16:0/20:4), 1-stearoyl-2-docosa-hexaenoyl-*sn*-glycero-3-phosphocholine (PC 18:0/22:6), 1-palmitoyl-2-oleoyl-*sn*-glycero-3-phosphocholine (PC 16:0/18:1), 1-octadecanoyl-2-(5Z,8Z,11Z,14Z,17Z-eicosapentaenoyl)-*sn*-glycero-3-phosphocholine (PC 18:0/20:5), 1-palmitoyl-2-docosahexaenoyl-*sn*-glycero-3-phosphoethanolamine (PE 16:0/22:6), 1,2-didocosahexaenoyl-*sn*-glycero-3-phosphoethanol-amine (PE 22:6/22:6) and 1-stearoyl-2-docosahexaenoyl-*sn*-glycero-3-phosphoethanolamine (PE 18:0/22:6), and porcine brain sphingomyelins were purchased from Avanti Polar Lipids, Inc. The stock solutions of these standards were prepared in chloroform. Two standard mixtures containing 10 μg/mL of the six PC species and the three PE species were prepared by dilution in methanol/acetonitrile (60:40, v/v). HPLC grade acetonitrile and LC–MS grade methanol were purchased from Merck (Darmstadt, Germany) and Sigma–Aldrich (St Louis, MO, USA), respectively.

Total lipids were extracted from mouse and cod brain samples by the Folch principle [26]. Briefly, samples were homogenized in chloroform/methanol (2:1, v/v), thoroughly vortex-mixed and filtered on Büchner funnel. Cod Brain extracts were washed with 0.2 volumes of 0.88% KCl and the water phase was discarded. The final extracts were evaporated to dryness and dissolved in 2 mL chloroform. An aliquot of 500 μL brain sample was taken out from this extract and dissolved in 500 μL methanol/acetonitrile (60:40, v/v) for the analysis of LC–MS.

3.2. LC–MS analysis

LC–MS analyses were carried out by using a 1100 series LC (Agilent) with a binary pump, autosampler, thermostatted column compartment connected to a Micromass Quattro MS equipped with an electrospray interface (Waters, Manchester, UK). The system was controlled by the MassLynx Software (Waters).

A reversed phase 50 mm × 2.1 mm ACE 5 C_{18} column with 5 μm particles (Advanced Chromatography Technologies, Aberdeen, UK), was used for the separations, and the column was kept at 35 °C. The LC conditions were adapted from [27]. Methanol/acetonitrile/water, 45:30:25 by volume, (Solvent A) and methanol/acetonitrile, 60:40 by volume (Solvent B) were used as mobile phases and both Solvent A and B contained 2.5 mM ammonium acetate (Sigma–Aldrich) and 10 μM serine (Sigma–Aldrich). The gradient program started at 40% B and increased to 100% B in 15 min, held for 45 min and returned to the initial condition in 1 min. The equilibration time between the injections was 9 min.

The ion source parameters were optimized by using both PC and PE standards. The ion source operated in positive mode, the source temperature was set to 150 °C and desolvation temperature was 400 °C. Nitrogen was used as curtain gas and argon was used as collision gas. PC species were detected by using PIS for *m*/*z* 184 with the collision energy of 45 eV and scanning for *m*/*z* 620 to 965, while PE species were monitored by using NLS for *m*/*z* 141 with the collision energy of 35 eV, and scanning in the range of *m*/*z* 575 to 920. The LC–MS raw data were exported to the self-describing, machine-independent data format, NetCDF (www.unidata.ucar.edu) by the DataBridge tool of MassLynx 4.0 Software.

3.3. Fatty acid analyses

Fatty acid methyl esters were prepared by as described in [28] and analyzed by GC-FID. Mouse brain samples were analyzed on a BPX-70 (SGE, Ringwood, Australia) using conditions described in [29] and cod brain samples were analyzed on a BP-20 column (SGE) using conditions described in [28]. In both cases empirical response factors calculated from the reference mixtures GLC463 or GLC-793 (Nu-Chek prep, Elysian, MN, USA) were applied for correcting the chromatographic areas, and results were expressed as percent of total fatty acids.

3.4. Software

The described algorithm was implemented in an in-house written program, Chrombox D 12-09 (www.chrombox.org) running under Matlab (Natick, MA, USA). NetCDF files with LC–MS raw data were read into Chrombox D and masses were binned to unit resolution with mass offsets of +0.2 Da and −0.1 Da for PC and PE data respectively. This ensured that the masses in the PC spectra were rounded upwards and masses of PE spectra were rounded downwards. Theoretical spectra were calculated with high resolution (4 decimals) in step 3 of the algorithm and then binned to unit resolution with offsets of +0.2 Da and −0.3 Da for PC and PE, respectively.

The following list of fatty acids was applied in step 2 of the algorithm: 12:0, 14:0, 14:1, 15:0, 16:0, 16:1, 17:0, 17:1, 18:0, 18:1, 18:2, 18:3, 18:4, 19:0, 19:1, 20:0, 20:1, 20:2, 20:3, 20:4, 20:5, 22:0, 22:1, 22:2, 22:3, 22:4, 22:5, 22:6, 24:0 and 24:1. This list of fatty acids will calculate 133 possible compounds in each lipid class, varying in number of carbon atoms from 24 to 48 and total number of double bonds from 0 to 12 in the two acyl chains. The threshold described in step 4 of the algorithm was set to 2% of the base peak. Since the

list of fatty acids contains fatty acids with odd-numbered carbon chains, the filter in step 5 was active in the algorithm. A flat spectral baseline was added to the spectra in $\mathbf{S}^T$, as described for steps 6 and 9 in the algorithm. After the first calculation the results were recalculated excluding compounds with less than 3% relative to the most abundant PC molecule, or less than 2% of the most abundant PE molecule. In the case of PC analysis in mouse brain, theoretical spectra of PC based SM were also calculated together with ordinary PC in step 2 of the algorithm. The ranges of chain lengths and number of double bonds in both the sphingoid bases and the fatty acids in the SM were the same as specified above.

4. Results and discussion

4.1. Analysis of PC in cod brain

The performance of the algorithm was tested by reference mixtures as well as biological samples such as cod brain and mouse brain. Results for the reference mixtures are given in supplementary material. Results for the brain extracts are described and discussed below. The total spectrum shown in Fig. 2a was extracted from the retention time range 15–46 min. The estimated baseline of the total spectrum is marked by a horizontal green line. The threshold value of the baseline described in step 4 in the algorithm is marked by the horizontal red line. Green bars are the masses in common with theoretical masses that remain in $\mathbf{S}^T$ after step 4, while red bars are masses that were above the threshold but not present in the theoretical spectra calculated in step 3. Other masses are shown in blue.

As can be seen in Fig. 2a, the total mass spectrum is quite complicated with the majority of the signals in the mass region m/z 700–900. Only a few ions above the threshold value were not accounted for by the spectra in $\mathbf{S}^T$. All of these were of minor abundance. With the complexity of the total mass spectrum there is significant overlap of the isotopic patterns of the individual compounds that is handled by the regression as explained in the theory section.

The amounts of the different compounds after resolution are shown by the bar plot in Fig. 2b. This is a plot of the values in $\mathbf{c}$ after application of Eq. (2), excluding the baseline signal that is also present in $\mathbf{c}$. The numbers in brackets are the ECN values of the compounds. The bar plot reveals that the main abundant PC species are PC 34:1, PC 36:1, PC 38:6 and PC 42:2, which are probably constituted by the following fatty acyl combinations, *i.e.*, 16:0/18:1, 18:0/18:1 or 16:0/20:1, 16:0/22:6 or 18:1/20:5 and 18:1/24:1, respectively. A full list of the identified compounds with possible fatty acid combinations are given as supplementary material in Table S1. These results are in close accordance with those reported previously [30–32], where the fatty acids or PC species compositions from cod brain were studied. The fatty acid combination also fits well with the fatty acid composition of the extracts obtained from the GC analysis (Table 1), which shows that 18:1, 22:6, 16:0, 18:0, 24:1, 20:5, 20:1 are the major fatty acids in the extracts. However, it is emphasized that the results in Table 1 are the fatty acid composition in the crude extract and that the composition in the different lipid classes will vary [30,32].

The result from the validation (algorithm step 8) is illustrated in Fig. 2c, where the abundances in $\mathbf{x}_{val}^T$ (Eq. (3)) are plotted against the corresponding masses from the original $\mathbf{x}^T$ shown in Fig. 2a. It can be seen that the original sum spectrum is accounted for with high accuracy by the spectrum calculated from the regression coefficients in $\mathbf{c}$ and the theoretical spectra in $\mathbf{S}^T$.

The result from the chromatographic resolution, as explained in step 9 of the algorithm gives additional information about the identity of the compounds. The data matrix $\mathbf{X}$, resolved profiles

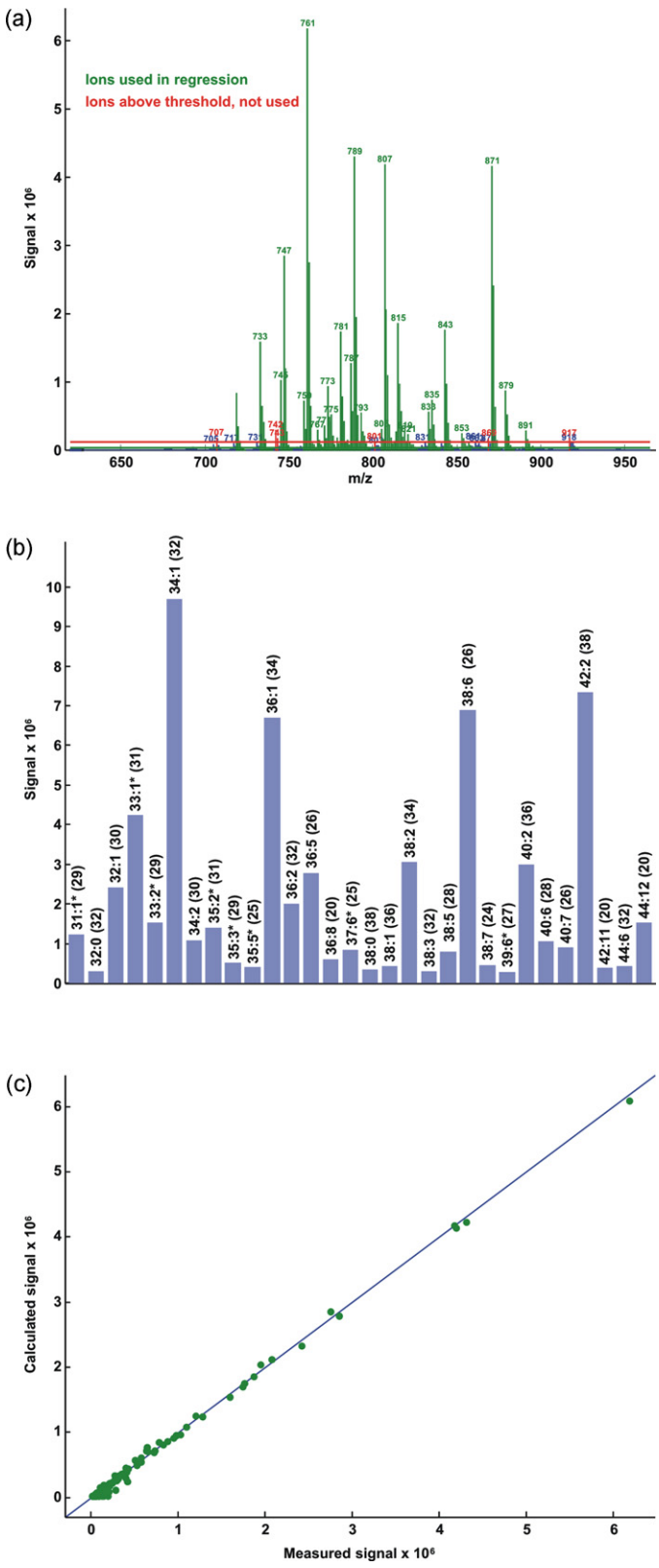

Fig. 2. Analysis of PC species from cod brain extracts. (a) The sum spectrum. Green bars are the masses used by the algorithm, red bars are other masses above a threshold marked by the horizontal red line, the horizontal green line is the estimated baseline; (b) Identified PC species with their pseudo concentrations showed by *y*-axis. Numbers in brackets are ECN values; (c) Validation of the results (predicted versus measured when the green masses in the total spectrum was reconstructed from the calculated solution). (For interpretation of the references to color in this figure legend, the reader is referred to the web version of the article.)

Table 1
Mass fraction of fatty acids (g/100 g) in cod brain and mouse brain samples. Fatty acids that were above 0.1% in one of the samples are reported.

	Cod brain	Mouse brain
14:0	0.53	0.15
16:0	14.42	23.28
16:1[a]	3.17	0.94
17:0	0.35	0.12
17:1	0.58	<0.01
18:0	9.22	20.83
18:1[b]	27.01	17.76
18:2 n-6	0.33	0.55
20:0	0.14	0.25
20:1[b]	3.32	1.17
20:2 n-6	0.19	0.16
20:3 n-6	0.07	0.42
20:4 n-3	0.27	<0.01
20:4 n-6	0.66	10.71
20:5 n-3	6.44	<0.01
22:0	0.16	0.31
22:1[b]	1.52	<0.01
22:2 n-6	0.10	<0.01
22:4 n-6	0.15	2.56
22:5 n-3	0.95	<0.01
22:6 n-3	21.26	19.12
24:0	0.37	0.51
24:1[b]	8.58	1.16

[a] Basically n-7 isomer.
[b] Basically n-9 isomer.

C (Eq. (4)) and residuals **R** (Eq. (5)) are shown on equal scales in Fig. 3a–c, respectively. The signals in **C** are larger than the signals in **X** because **C** contains the sum of all isotopomers of each PC species. Irregularly shaped peaks or double peaks should be expected since several combinations of fatty acids may give PC species with the same masses.

The residuals are small compared to the magnitudes in **C** and **X**, showing that the majority of variance in **X** has been accounted for in all parts of the chromatograms. The majority of the variance in **X** are spikes with short frequencies in the regions where there are chromatographic peaks, probably arising from heteroscedastic noise in **X**. But some of the ions in **R** show similarity to chromatographic profiles, such as m/z 779, 783 and 814, indicating that there may be minor compounds that are not accounted for by the spectra in $\mathbf{S}^T$.

The retention of PC species in reverse phase LC follows their ECN values due to specific hydrophobic interaction of their fatty acyl chains with the alkyl ligand of the stationary phase [33]. This means that the PC species having the same ECN values are basically in the same retention time region and the PC species are gradually eluted with increasing ECN values. This rule can be used to assist the identification of the compounds since false identifications based on the spectra alone may arise from the presence of minor compounds such as ether-linked plasmanyl or plasmenyl PC species (plasmalogens). Most of the ether-linked species can be distinguished from the diacyl PC species through the bar plot (Fig. 2b) or the resolved chromatographic profiles (Fig. 3b). Common plasmalogens has the same integer masses as ordinary PC with odd number of carbon atoms, and it has been shown that ether-linked PC species elute later than their diacyl counterparts on a reverse phase column [7,34].

The most abundant compounds identified as PC with odd number of carbon atoms are 33:1, 35:2, 31:1 and 33:2, which have the same integer masses as 34:0, 36:1, 32:0 and 34:1 plasmalogens, respectively. These are among the most common and abundant PC plasmalogens previously reported in brain [35]. They also elute later than what should be expected from their calculated ECN number, which should be expected according to [7,34] if they are plasmalogens.

There are two peaks corresponding to PC 33:2, where one has the expected retention time for an ordinary PC with odd number of carbon atoms, and one peak has stronger retention indicating that it is the 34:1 plasmalogen. PC 39:6 also has correct ECN value for ordinary PC and can be explained by the fatty acid combination 17:0 and 22:6 (Table 1). The remaining compounds reported as PC with odd number of carbon atoms (37:6, 35:3, 35:5) can either be explained by previously reported plasmalogens in brain [35] or by the abundant 22:6 or 22:5 fatty acids combined with ether linked C16 or C18 alkenyl or alkanyl chains.

4.2. Analysis of PE in cod brain

The results for the PE analysis are presented in Figs. 4 and 5. The extracted total mass spectrum from the retention time range between 16 and 31 min (Fig. 4a) are simpler than the corresponding spectrum for PC.

Most of the ions are concentrated in the mass region m/z 700–850 and a few minor ions above the threshold value marked by red were not accounted in the spectrum $\mathbf{S}^T$. The most abundant ions, m/z 836, 764, 792 and 790 correspond to the base peaks of PE 44:12, PE 38:6, PE 40:6, PE 40:7, respectively, Fig. 4b. Based on the fatty acid composition in Table 1, it is likely that the dominating PE species have the following fatty acyl combinations: 22:6/22:6 for PE 44:12, 16:0/22:6 or 18:1/20:5 for PE 38:6, 18:0/22:6, 18:1/22:5 or 20:1/20:5 for PE 40:6 and 18:1/22:6 for PE 40:7. A full list of proposed structures is given in the supplementary material, Table S2.

This presence of mainly 22:6, 18:1, 16:0 and 18:0 containing PE species coincides well with other studies [30–32]. The result from the validation (algorithm step 8) shown in Fig. 4c reveals that the deviation between the predicted and measured total spectrum is small, and there are only a few minor masses contributing to the total signal that are not accounted for.

The results from the chromatographic resolution after the application of algorithm step 9 are given in Fig. 5. Similar to PC, the elution pattern of diacyl PE and ether-linked PE species can be used as a diagnostic tool for the accurate identification of these species. It is worth noting that the resolved chromatogram (Fig. 5b) indicates the presence of several isobaric species which have the same mass but different fatty acyl combinations. PE 38:6 has two closely eluting chromatographic peaks, possibly consisting of 16:0/22:6 and 18:1/20:5. Similarly, PE 40:6 consists of three chromatographic peaks which probably correspond to 18:0/22:6, 18:1/22:5 and 20:1/20:5. The resolved PE chromatogram (Fig. 5b) only show four minor peaks with odd number of carbon atoms that may arise from ether-linked species [36].

4.3. Mammalian brain lipids

The bar plots from the mouse brain analysis are presented in Fig. 6 and the proposed identity of the compounds are listed in the supplementary material, Tables S3 and S4. The main mouse brain PC species were 34:1, 36:1, 32:0 and 38:6, constituted by 16:0/18:1, 18:0/18:1 or 16:0/20:1, 16:0/16:0 and 16:0/22:6, respectively (Fig. 6a). The same four compounds have previously been reported to be the most abundant PC species in mouse brain [37]. Although the mouse brain PC profile is less complex than the corresponding cod brain profile, they share several abundant species, such as PC 34:1 (16:0/18:1), 36:1 (18:0/18:1 or 16:0/20:1) and 38:6 (16:0/22:6).

The results for mouse brain PC were calculated with the function for SM active in step 2 of the algorithm, in addition to the function for ordinary PC. Because SM have different number of N atoms than ordinary PC they cannot have similar spectra. They are therefore less problematic to analyze together with PC than for instance

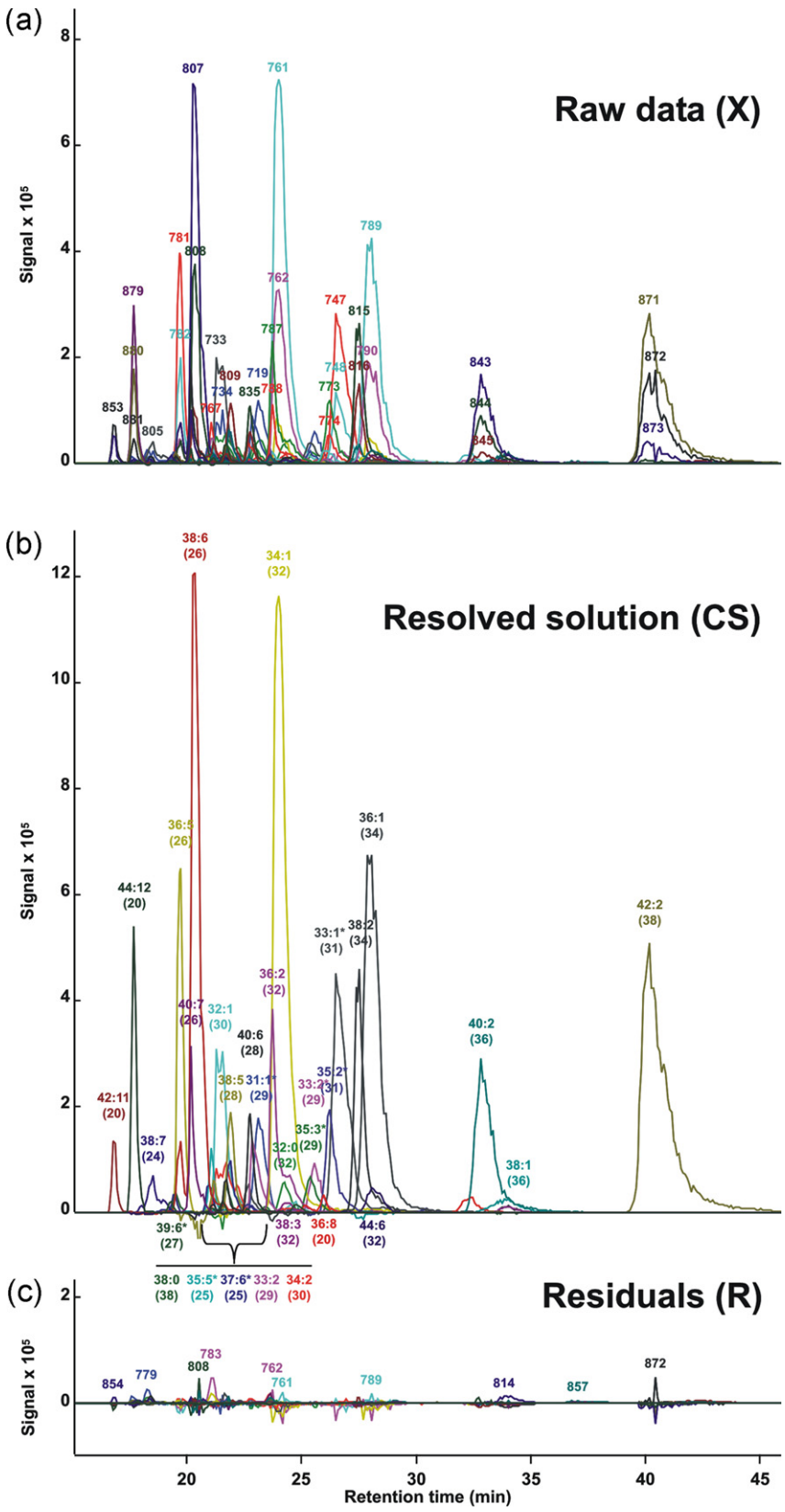

Fig. 3. The plot of raw data matrix **X** (a), resolved chromatographic profiles **C** (b) and residuals **R** after resolution (c) of PC species from cod brain extracts. (a–c) are shown on equal scales.

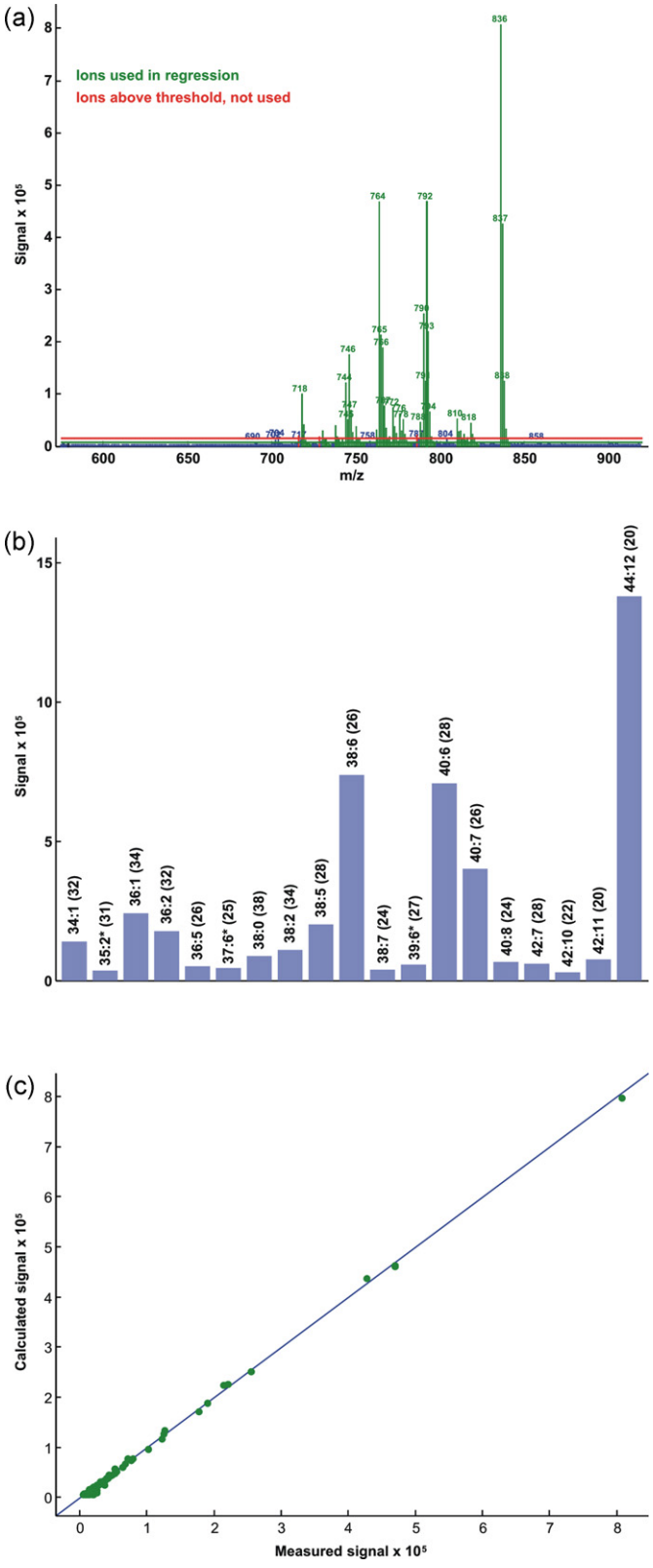

Fig. 4. Analysis of PE species from cod brain extracts. (a) The sum spectrum. Green bars are the masses used by the algorithm, red bars are other masses above a threshold marked by the horizontal red line, the horizontal green line is the estimated baseline; (b) Identified PE species with their pseudo concentrations showed by *y*-axis. Numbers in brackets are ECN values; (c) Validation of the results (predicted versus measured when the green masses in the total spectrum was reconstructed from the calculated solution). (For interpretation of the references to color in this figure legend, the reader is referred to the web version of the article.)

the plasmalogens. Only three compounds were detected above the threshold of the 133 theoretically possible SM molecular formulas that were calculated from the list of fatty acids. These were SM 36:1, SM 36:2 and SM 42:2. All three have previously been reported to be among the most abundant SM in mammalian brain with 36:1 and 42:2 as the two most abundant [38,39].

It should be emphasized that our extraction methods and LC–MS parameters are not optimized for SM, so the levels shown in Fig. 6a may not be representative for the ratio between ordinary SM and ordinary PC. The sum of SM molecules is approximately 7% of the sum of PC. Ratios of SM to PC in mouse brain have been reported to be typically around 10% [40].

Results for an analysis of a porcine brain SM reference mixture analyzed by the same method are reported as supplementary material (Table S5 and Figures S5 and S6). No ordinary PC was detected in this sample. The levels of different SM agreed well with a previous report on the bovine brain SM [39]. Two of the detected compounds have deviating ECN values indicating that they are not ordinary SM or PC. Of the remaining 14 compounds, 12 were reported in the previous work [39], and only one of the abundant compounds (>1% relative to largest) reported in this work was not detected above the threshold (SM 43:1).

The bar plot of mouse brain PE (Fig. 6b) suggests that the main species are 40:6, 38:4, 38:6 and 36:1, constituted by 18:0/22:6, 18:0/20:4 or 16:0/22:4, 16:0/22:6 and 18:0/18:1 or 16:0/20:1, respectively. The main trends in the obtained results are in accordance with previous works [41–43].

In the fatty acids profiles of the extracts (Table 1), the most striking difference between cod and mouse brains can be seen in the levels of the polyunsaturated fatty acids 20:4 and 20:5, and partly also in the elongated 22:4 and 22:5. While 20:5 and 22:5 are high in cod brain these are absent in the mouse brain, and 20:4 and 22:4 that are found in high levels in mouse brain are in very low levels in the cod brain. This is also reflected in the results found from the LC–MS analyses. Except from PE 42:10 (20:4/22:6), which was found in minor amounts in cod brain, 20:4 and 22:4 seem absent in PC and PE from cod brain. Similarly, 20:5 and 22:5 are absent in the mouse brain PE and PC.

4.4. Discussion of the algorithm

The algorithm as presented in Section 2.2 can be extended or modified in several ways. One obvious way to adapt the procedure to different types of samples is to modify the list of fatty acids to contain only fatty acids that are present in the samples above a certain threshold. Step 2 in the algorithm can generate spectra of more than one lipid class, which was used in the analysis of mouse brain PC. In addition to specifying sphingolipids in cases where this is relevant, one can also include spectra of other compounds that may be detected by the same methods as used for the main phospholipid classes, such as lyso-phospholipids or plasmalogens. However, such an extension of step 2 may also require modifications of the filter for spectral similarity in step 5. Alternatively, step 2 can be omitted and replaced by a predefined list of molecular formulas suitable to the sample type of interest. This will probably give higher numerical stability and better precision in analyses of large sequences. Similarly, both step 2 and 3 can be replaced by a predefined list of spectra.

We have only applied the methodology with unit resolution mass spectra, but in theory the procedure can be adapted also to high resolution instruments. However, instruments capable of running PIS and NLS with high resolution are few since high resolution would be required in the first mass filter.

Compared to other ionization techniques electrospray ionization usually leads to quite noisy data, which is something that can also be seen in the raw data profiles in Figs. 3a and 5a. However,

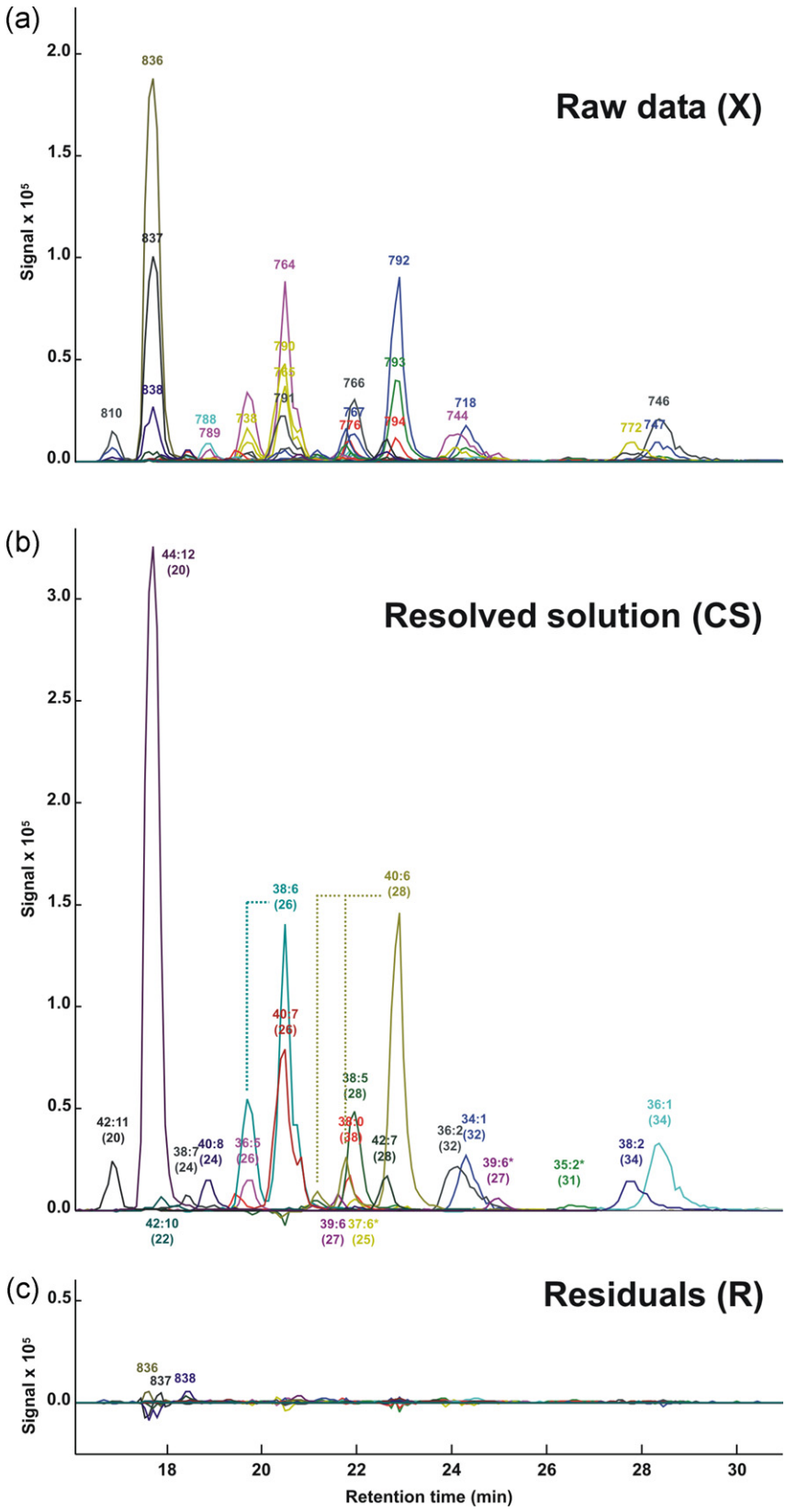

Fig. 5. The plot of raw data matrix **X** (a), resolved chromatographic profiles **C** (b) and residuals **R** after resolution (c) of PE species from cod brain extracts. (a–c) are shown on equal scales.

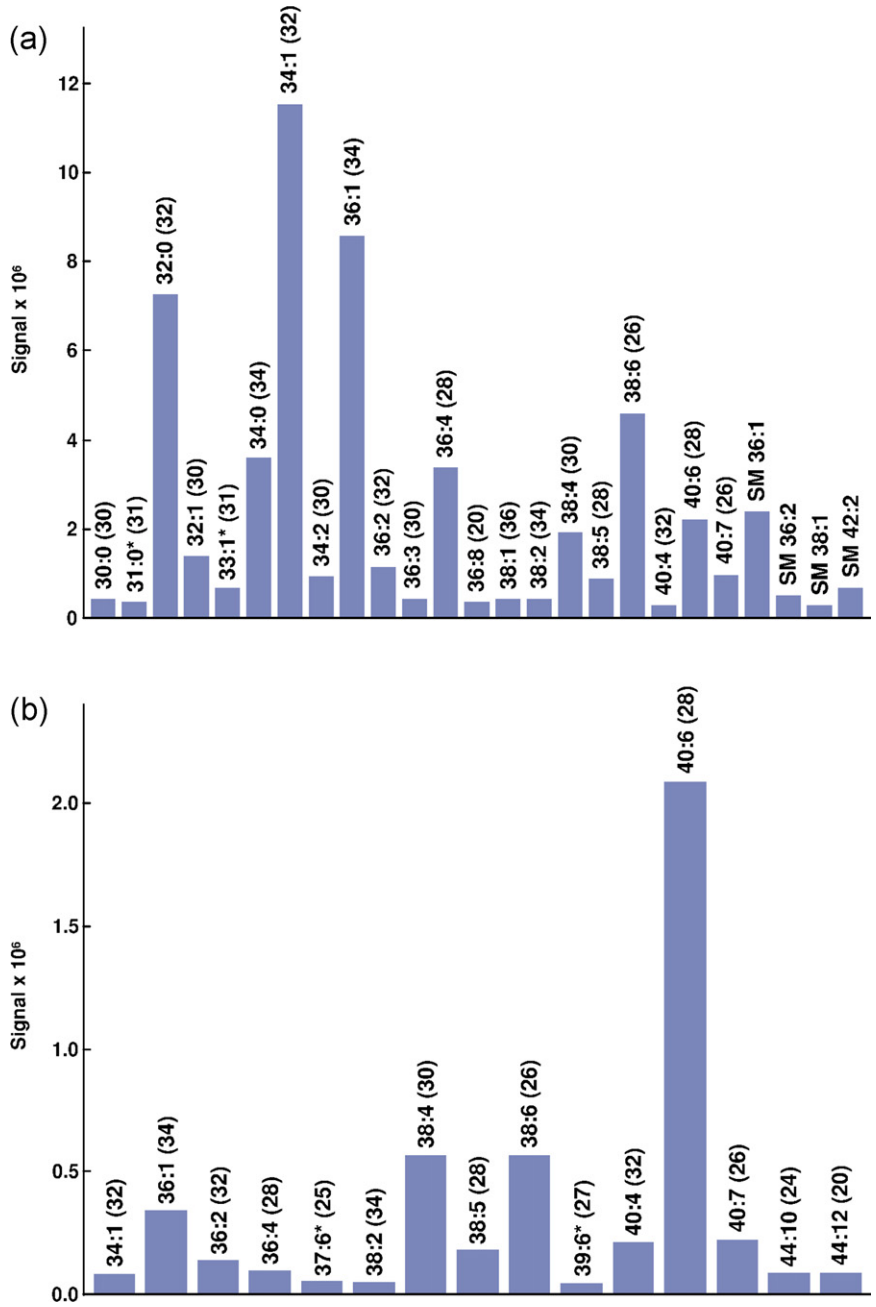

Fig. 6. Identified (a) PC, SM and (b) PE species from mouse brain extracts.

since the noise is basically caused by processes in the ion source, such as instable ionization and ion suppression, the majority of the noise in the data is added before the mass filter. With reference to Eqs. (4) and (5) one can say that the noise in **X** stems basically from **C** and not from $\mathbf{S}^T$. This is the reason for the quite small residuals even though the data are noisy.

The noise in mass spectrometry is usually heteroscedastic, where absolute noise in the signals increase with the signal strength [44]. This may typically affect the accuracy of quantification of minor compounds that have ions in common with major compounds in the total spectrum. This is a problem related to the structure in the raw data, so it will be equally problematic also with other methods for quantification and isotope correction that is based on a single mass spectrum. But if minor peaks are chromatographically separated from larger peaks that share some of the ions (the source of the noise) they will not be influenced in the same way. In many cases it may therefore be better to base the quantification on integrated profiles of **C** from Eq. (4) than on the regression coefficients, **c**, from Eq. (2). Alternatively, the algorithm may be used on sections of the chromatogram. In the current version of the applied program there is no possibility to integrate the profiles, but they can be exported and quantified for instance by Chrombox C (www.chrombox.org) also running under Matlab.

Noise will typically also lead to detection of a large number of minor compounds and also some compounds with small negative values in **c**, depending on the threshold selected in step 4. These can be removed by recalculating only with compounds that had signal above a certain value. However, since the signals from compounds that are omitted from the recalculation are still present in the

measured spectrum, $\mathbf{x}^T$, they may influence accuracy of compounds that share some of the masses. Setting the threshold for the recalculation too high may therefore have negative effect on the accuracy, which will be seen in the $\mathbf{x}^T$ versus $\mathbf{x}^T_{val}$ plots. To facilitate presentation of the data, we have in this work used higher thresholds than what we would have selected if we wanted maximal accuracy for minor compounds. Another way to avoid negative values is to use a regression that constrains $\mathbf{c}$ to have only non-negative values. This is an option in the current version of the program, but it should be used with care since negative values may be of diagnostic importance.

The filtering of similar ions in step 5 of the algorithm is also implemented in the software as an option. If the filter is turned off, similar spectra will be flagged and it is possible to recalculate after manual selection of one of the similar compounds. The threshold value for the correlation between spectra of 0.9 works fine for the data presented used in this work, but it is emphasized that a suitable level may depend on the amount of noise in the data.

In theory it is possible to apply similar methodology on other compounds. But the methodology requires a reasonable fit between measured and theoretically calculated spectra, as well as limited abundance of interferents that are not accounted for by the theoretical spectra. Similar methodology has for instance been applied for deconvolution of petroleum compounds [45] and selenides [46] analyzed by high-resolution mass spectrometry.

4.5. Comparison with alternative methods

Several tools for analysis of data from direct infusion MS or LC–MS of lipids have been described in the scientific literature. These include software such as LipidProfiler [14], LipidInspector [15], LipidQA [16], Fatty acid Analysis Tool (FAAT) [17], LipidXplorer [18], LIMSA [20], MZmine2 [21], Profiler-Merger-Viewer [22] and Lipid Data Analyzer (LDA) [23]. The various programs differ widely in scope and flexibility. Some tools are basically designed for direct infusion MS [14–18], and other are designed for LC–MS [20–23]. However, programs designed for LC–MS may not take full advantage of the LC separation, and some of the direct infusion methods may handle spectra extracted from LC–MS chromatograms, so there is no clear distinction between these two classes. The methods differ in requirements for mass spectral resolution and whether centroided or full profile spectra are applied. Some methods are claimed to handle both high and low resolution MS [14–16,18,21]. The various tools also have different scopes. While some tools aim at identification and quantitation of the signal generated from each compound (like the methodology described in this paper) other have built-in modules for visualization, statistics, and absolute quantitation using standards.

The data from the experiments described in Section 3 could be analyzed by LIMSA [20] and MZmine2 [21]. Quantitative results were evaluated by comparing the 19 compounds that were found above 1% in the cod brain sample (Supplementary material, Table S1). There was a large degree of correlation with R^2 of 0.9993 and 0.9964 when the values from the LSSR algorithm were compared against LIMSA and MZmine2, respectively. However, both LIMSA and MZmine2 reported a large number of compounds (>50) that were found in very small levels. These were not present above the noise level in the raw data. The same problem was also seen with the PC reference mixture that contains only 6 compounds. This is probably caused by differences in how the background signals in the spectra are handled by the algorithms. LIMSA and MZmine also failed on identification of some of the abundant compounds. In LIMSA this problem can be solved by editing the lists that specifies the compounds that may be available in a sample. Some of the typical marine compounds containing 22:5 n-3 or 22:6 n-3 were not specified in the original peak lists. In MZmine2 there was a tendency that the compounds with highly unsaturated fatty acids were identified as compounds with odd number of carbon atoms, *e.g.* PC 44:12 was assigned as PC 43:5 that has the same mass in low resolution spectra. As explained in the theory section, this conflict is not a problem when the resolution is better than 0.1 Da. The possibility to apply a filter similar to that described as step 5 in the algorithm (Section 2.3) or any other means of giving priority to one of the conflicting compounds could make MZmine2 more suitable for low resolution spectra.

There is a large variety in software tools for lipid analysis and in the quality of the data produced on different instrumentation, and it is challenging to evaluate from published literature which tool that would give the best performance in a particular case. The only advice we would like to give on the choice between the different tools is to test them thoroughly with data from the application they are intended to be used for. Many tools specify lists of compounds that are expected to be present. Particular attention should be paid to these lists and if they cover the content of the samples. It is often possible to exclude compounds from these lists, for instance in cases where pre-separation steps or selective MS scan modes are applied, or if knowledge about the sample type tells that certain compounds cannot be present. Constraining the lists to compounds that can be expected in the samples reduces the risk of incorrect identifications and may lead to more accurate and precise quantitative results.

5. Conclusions

A methodology for automated identification and quantification of molecular forms of PC and PE analyzed by respectively neutral loss scan and precursor ion scan in electrospray ionization LC–MS has been proposed. The methodology is based on calculation of theoretical spectra of the isotope distribution of possible compounds defined by a list of fatty acids, and subsequent resolution of the raw data by least squares regression.

The described algorithm was able to resolve PC and PE species of reference mixtures, porcine brain SM and extracts of brain lipids. The built-in validation approach showed that the raw data signals were accounted for, and the obtained results were reasonable considering the fatty acid profile of the extracts and results previously reported in the literature.

The methodology can be applied on a single sum-spectrum, and may therefore be feasible for shotgun lipidomics, but resolution of chromatographic raw data may give additional information about the identity and amounts of the individual compounds. The flexibility of the algorithm allows it to be expanded to other compound classes in the future.

Acknowledgements

Mouse brain was obtained from Haukeland University Hospital and National Institute of Nutrition and Seafood Research (Bergen, Norway). Cod brain was provided by Institute of Marine Research, Bergen, Norway.

Appendix A. Supplementary data

Supplementary data associated with this article can be found, in the online version, at http://dx.doi.org/10.1016/j.chroma.2012.12.070.

References

[1] M. Pulfer, R.C. Murphy, Mass Spectrom. Rev. 22 (2003) 332.

[2] V. Frisardi, F. Panza, D. Seripa, T. Farooqui, A.A. Farooqui, Prog. Lipid Res. 50 (2011) 313.
[3] A.A. Farooqui, L.A. Horrocks, T. Farooqui, Chem. Phys. Lipids 106 (2000) 1.
[4] D.F. Horrobin, C.N. Bennett, Prostag. Leukotr. Ess. 60 (1999) 217.
[5] X.L. Han, R.W. Gross, Mass Spectrom. Rev. 24 (2005) 367.
[6] B.L. Peterson, B.S. Cummings, Biomed. Chromatogr. 20 (2006) 227.
[7] J.F.H.M. Brouwers, E.A.A.M. Vernooij, A.G.M. Tielens, L.M.G. van Golde, J. Lipid Res. 40 (1999) 164.
[8] H.Y. Kim, T.C.L. Wang, Y.C. Ma, Anal. Chem. 66 (1994) 3977.
[9] J.F.H.M. Brouwers, B.M. Gadella, L.M.G. van Golde, A.G.M. Tielens, J. Lipid Res. 39 (1998) 344.
[10] P.S. Niemela, S. Castillo, M. Sysi-Aho, M. Oresic, J. Chromatogr. B 877 (2009) 2855.
[11] W.D. Lehmann, M. Koester, G. Erben, D. Keppler, Anal. Biochem. 246 (1997) 102.
[12] N. Navas-Iglesias, A. Carrasco-Pancorbo, L. Cuadros-Rodriguez, TrAC-Trends Anal. Chem. 28 (2009) 393.
[13] B. Brügger, G. Erben, R. Sandhoff, F.T. Wieland, W.D. Lehmann, Proc. Natl. Acad. Sci. U.S.A. 94 (1997) 2339.
[14] C.S. Ejsing, E. Duchoslav, J. Sampaio, K. Simons, R. Bonner, C. Thiele, K. Ekroos, A. Shevchenko, Anal. Chem. 78 (2006) 6202.
[15] D. Schwudke, J. Oegema, L. Burton, E. Entchev, J.T. Hannich, C.S. Ejsing, T. Kurzchalia, A. Shevchenko, Anal. Chem. 78 (2006) 585.
[16] H. Song, F.F. Hsu, J. Ladenson, J. Turk, J. Am. Soc. Mass Spectrom. 18 (2007) 1848.
[17] M.D. Leavell, J.A. Leary, Anal. Chem. 78 (2006) 5497.
[18] R. Herzog, K. Schuhmann, D. Schwudke, J.L. Sampaio, S.R. Bornstein, M. Schroeder, A. Shevchenko, PLoS One 7 (2012) e29851.
[19] J.F. Brouwers, Biochim. Biophys. Acta 1811 (2011) 763.
[20] P. Haimi, A. Uphoff, M. Hermansson, P. Somerharju, Anal. Chem. 78 (2006) 8324.
[21] T. Pluskal, S. Castillo, A. Villar-Briones, M. Oresic, BMC Bioinformatics 11 (2010) 395.
[22] E.M. Hein, B. Bodeker, J. Nolte, H. Hayen, Rapid Commun. Mass Spectrom. 24 (2010) 2083.
[23] J. Hartler, M. Trotzmuller, C. Chitraju, F. Spener, H.C. Kofeler, G.G. Thallinger, Bioinformatics 27 (2011) 572.
[24] Anon., J. Lipid Res. 19 (1978) 114.
[25] E.R. Malinowski, Factor Analysis in Chemistry, 3rd ed., Wiley, New York, 2002.
[26] J. Folch, M. Lees, G.H.S. Stanley, J. Biol. Chem. 226 (1957) 497.
[27] K. Retra, O.B. Bleijerveld, R.A. van Gesteil, A.G.M. Tielens, J.J. van Hellemond, J.F. Brouwers, Rapid Commun. Mass Spectrom. 22 (2008) 1853.
[28] S. Meier, S.A. Mjøs, H. Joensen, O. Grahl-Nielsen, J. Chromatogr. A 1104 (2006) 291.
[29] C. Sciotto, S.A. Mjøs, Lipids 47 (2012) 659.
[30] M.V. Bell, J.R. Dick, Lipids 26 (1991) 565.
[31] S. Meier, T.C. Andersen, K. Lind-Larsen, A. Svardal, H. Holmsen, Comp. Biochem. Physiol. C 145 (2007) 420.
[32] D.R. Tocher, D.G. Harvie, Fish Physiol. Biochem. 5 (1988) 229.
[33] M. Smith, F.B. Jungalwala, J. Lipid Res. 22 (1981) 697.
[34] S. Ramanadham, A. Bohrer, R.W. Gross, J. Turk, Biochemistry 32 (1993) 13499.
[35] A. Üllen, G. Fauler, H. Kofeler, S. Waltl, C. Nusshold, E. Bernhart, H. Reicher, H.J. Leis, A. Wintersperger, E. Malle, W. Sattler, Free Radic. Biol. Med. 49 (2010) 1655.
[36] K.A. Kayganich, R.C. Murphy, Anal. Chem. 64 (1992) 2965.
[37] Y. Sugiura, Y. Konishi, N. Zaima, S. Kajihara, H. Nakanishi, R. Taguchi, M. Setou, J. Lipid Res. 50 (2009) 1776.
[38] F.B. Jungalwala, V. Hayssen, J.M. Pasquini, R.H. Mccluer, J. Lipid Res. 20 (1979) 579.
[39] F.F. Hsu, J. Turk, J. Am. Soc. Mass Spectrom. 11 (2000) 437.
[40] H. Sakai, Y. Tanaka, M. Tanaka, N. Ban, K. Yamada, Y. Matsumura, D. Watanabe, M. Sasaki, T. Kita, N. Inagaki, J. Biol. Chem. 282 (2007) 19692.
[41] Y.C. Ma, H.Y. Kim, Anal. Biochem. 226 (1995) 293.
[42] M. Hermansson, A. Uphoff, R. Kakela, P. Somerharju, Anal. Chem. 77 (2005) 2166.
[43] V. Matyash, G. Liebisch, T.V. Kurzchalia, A. Shevchenko, D. Schwudke, J. Lipid Res. 49 (2008) 1137.
[44] X.N. Li, Y.Z. Liang, F.T. Chau, Chemom. Intell. Lab. Syst. 63 (2002) 139.
[45] S.G. Roussis, R. Proulx, Anal. Chem. 75 (2003) 1470.
[46] J. Meija, J.A. Caruso, Am. Soc. Mass Spectrom. 15 (2004) 654.